Article

Effects of Cosolvents and Crowding Agents on the Stability and Phase Transition Kinetics of the SynGAP/PSD-95 Condensate Model of Postsynaptic Densities

Hasan Cinar, Rosario Oliva, Haowei Wu, Mingjie Zhang, Hue Sun Chan, and Roland Winter*

Cite This: *J. Phys. Chem. B* 2022, 126, 1734−1741

Read Online

ACCESS | Metrics & More | Article Recommendations | Supporting Information

ABSTRACT: The SynGAP/PSD-95 binary protein system serves as a simple mimicry of postsynaptic densities (PSDs), which are protein assemblies based largely on liquid−liquid phase separation (LLPS), that are located underneath the plasma membrane of excitatory synapses. Surprisingly, the LLPS of the SynGAP/PSD-95 system is much more pressure sensitive than typical folded states of proteins or nucleic acids. It was found that phase-separated SynGAP/PSD-95 droplets dissolve into a homogeneous solution at a pressure of tens to hundred bar. Since organisms in the deep sea are exposed to pressures of up to ∼1000 bar, this observation suggests that deep-sea organisms must counteract the high pressure sensitivity of PSDs to avoid neurological impairment. We demonstrate here that the compatible osmolyte trimethyl-amine-*N*-oxide (TMAO) as well as macromolecular crowding agents at moderate concentrations can mitigate the deleterious effect of pressure on SynGAP/PSD-95 droplet stability, extending stable LLPS up to almost a kbar level. Moreover, the formation of SynGAP/PSD-95 droplets is a very rapid process that can be switched on and off in seconds. In contrast with the marked effects of the cosolutes on droplet stability, at the cosolutes' respective biologically relevant concentrations, their impact on the phase transformation kinetics is rather small. Only a high TMAO concentration results in a significant kinetic retardation of LLPS. Taken together, these findings offer new biophysical insights into the neurological effects of hydrostatic pressure. In particular, our results indicate how pressure-induced neurological disorders might be alleviated by upregulating certain cosolutes in the cellular milieu.
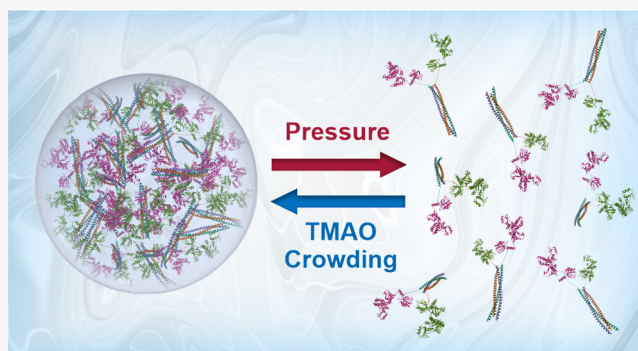
1. INTRODUCTION

Pressure embodies a fundamental thermodynamic state variable. Changes induced by pressure lead to alterations in equilibria and reaction rates not only in chemical but also in biological systems.[1−9] Organisms exhibit a variety of physiological changes when exposed to pressures that reach values of several hundreds to about thousand bar in the deep ocean.[4,5,12−14] In biological cells, there are many components that are very sensitive to pressure changes, including, in particular, lipid membranes, ion channels and transporters located in the membrane, and multi-subunit protein complexes, such as those of the cellular cytoskeleton.[5,10−12]

Synapses using ion channels and chemically activated receptors that regulate neurotransmission are particularly vulnerable to pressure exposure.[12−14] The changes in nervous system excitability and motor function that result from exposure of the central nervous system to pressure are referred to as high-pressure neurological syndrome (HPNS).[13−15] The biophysical and physiological basis of this syndrome is still largely unknown. One speculation is that it is caused by pressure effects on the kinetics of activation and inactivation of membrane-bound ion channels and receptors at the nerve

terminals. In other words, HPNS might originate from pressure-induced alterations in synaptic transmission and postsynaptic receptor functioning. In general, understanding the adaptations that allow bacteria, invertebrates, and some vertebrates to live under high hydrostatic pressure requires a comprehensive analysis of the structural and energetic features of proteins and other cellular components that operate under high pressure.

Here, we further explore a scenario that offers a tentative rationalization of neurological dysfunction at increased hydrostatic pressure. Eukaryotic cells, including neurons, need unique subcellular compartmentalization to function. These include membrane-bound organelles as well as membraneless organelles based largely on liquid−liquid phase separation (LLPS) of proteins and nucleic acids.[16−20] A prominent
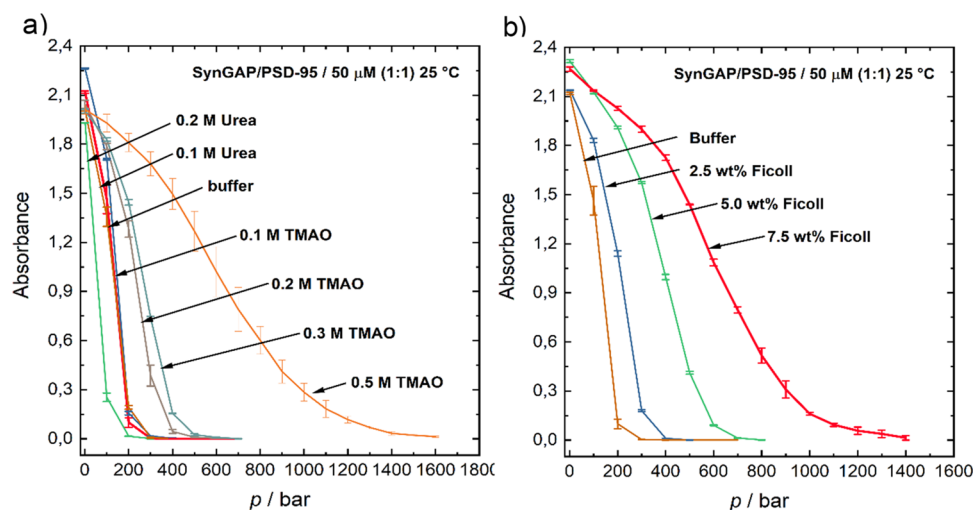
Figure 1. Representative UV/Vis absorption (turbidity) data at 400 nm of a 50 μM (1,1) solution of SynGAP/PSD-95 as a function of pressure (a) in buffer, 0.1−0.2 M urea and 0.1−0.5 M TMAO, and (b) in 2.5−7.5 wt % Ficoll at T = 25 °C. The absorption data were normalized to their maximum values. Data points are averages of three independent measurements.

example of neuron-specific membraneless organelles is postsynaptic density (PSD).[21−23] PSDs are protein-rich compartments situated beneath the postsynaptic membrane. They concentrate neurotransmitters and receptors and exchange small molecules and proteins with the surrounding cytoplasm. Two primary components of PSD are SynGAP and PSD-95, which together are capable of undergoing LLPS in vivo and in vitro.[21] Although biological PSDs contain many other protein components,[22] the behaviors of the simple SynGAP/PSD-95 model for PSD suggest that the PSD droplet phase is at least partially stabilized by intermolecular interactions between the folded PDZ domains of PSD-95 and a protein-binding motif of SynGAP.[24]

Recently, we and others observed that some proteins undergoing LLPS can be very pressure sensitive.[20,25−30] In some cases, such as γ-crystallin and the SynGAP/PSD-95 model of PSD, pressures of tens to hundred bar have been found to cause conversion from the phase-separated state to a homogeneous solution. Since organisms in the deep sea live at pressures up to about 1000 bar, this means that they must develop means to counteract this high pressure sensitivity of protein condensates to avoid functional impairment. It follows that the existence of life at great ocean depths indicates the need for specific genetics—which may include but is not limited to amino acid and nucleic acid sequences that encode for structures that are more stable under pressure—or general adaptive mechanisms. In light of the apparent pressure sensitivity of PSDs[27] and its possible relationship with HPNS,[15] this demand may be especially acute for the nervous system[10,12−14]

In this study, we focus on possible general adaptive mechanisms, namely whether upregulation of certain cellular components may be able to rescue PSDs from pressure-induced deterioration by using the SynGAP/PSD-95 system as a model PSD. As macromolecular crowding agents and cosolvents are common constituents of the cellular milieu and are known to affect the stability and conformational dynamics of biomolecular systems,[31,32] we studied the impact of macromolecular crowding as well as the cosolvents trimethylamine-N-oxide (TMAO) and urea on the stability of SynGAP/PSD-95 condensates. In general, the cellular

environment is very crowded with proteins, polysaccharides, smaller molecules, and membrane surfaces, all reducing the availability of space. In the present investigation, the 10 nm-sized nonionic synthetic polysaccharide Ficoll was used as a model for molecules that contribute to cellular macromolecular crowding. For cosolvents, we chose to study TMAO as a compatible osmolyte as it is upregulated in organisms living in the deep sea at high pressures up to several hundred bar.[33,34] For this reason, TMAO is also believed to serve as a pressure counteractant (denoted "piezolyte"),[34] and its physico-chemical properties and biological role have been studied extensively.[35−38] Urea as a cosolvent was also studied here for its generally opposite effects on biomolecular configurations compared to those of TMAO.[39,40] Elucidating the effects of TMAO on PSDs is also relevant to human physiology and disease. TMAO, the oxidation product of trimethylamine, is a hepatic metabolite of humans that originates from the gut microbiota catabolism of dietary nutrients. Relatively high concentrations of TMAO in the blood stream and cerebrospinal fluid have also been found in diabetics and in patients with cognitive impairment and dementia.[41−43] TMAO likely alters presynaptic and postsynaptic receptor expression; and it has been suggested that TMAO may cause deficits in expression levels of synaptic plasticity-related proteins such as PSD-95 and downregulate mTOR signaling.[41] These effects could have significant neurological ramifications as reduced expression of PSD-95 was found to induce cognitive and memory dysfunction.[41]

A fundamental difference between compartmentalization by lipid bilayer membranes and by LLPS is that biomolecular condensates can form and dissolve more rapidly in response to gradients in biomolecule concentrations or environmental stimuli. With this in mind, the kinetics of assembly and disassembly of biomolecular condensates is considered to be of central importance to their biological function. For this reason, we have also addressed the LLPS kinetics of the SynGAP/PSD-95 model system and the manner in which the kinetics is affected by the various cosolutes by using pressure-jump relaxation spectroscopy. Utilizing pressure as a physical probe, the pressure-jump method has several advantages over other techniques for studying the kinetics of phase transitions[5,48] in

that pressure is a very mild perturbing agent that acts instantaneously and uniformly (hence no additional mixing is needed) and that pressure-jumps can be applied in both phase transition directions (enhancing or attenuating LLPS) without changes in sample composition or thermal energy. Results of our investigations are detailed below.

2. RESULTS

2.1. UV/Vis and Light Microscopy Measurements: The Effect of Cosolutes on LLPS Formation under Pressure. Pressure-dependent UV/Vis absorption measurements were used to study the pressure-dependent LLPS behavior of the SynGAP/PSD-95 system at a concentration of 50 μM (1:1) in buffer and in different cosolvent solutions. SynGAP and PSD-95 were prepared following previously described procedures.[21,22] TMAO, one of the most potentially compatible osmolytes, and the macromolecular crowding agent Ficoll were used as stabilizing cosolvents; urea was employed as a prototypical destabilizing cosolvent. Liquid droplet formation upon LLPS was monitored by measuring the turbidity (i.e., apparent absorption) through light scattering at 400 nm with a UV/Vis spectrometer. The pressure-dependent measurements were performed using a home-built high-pressure optical cell with 10 mm-diameter-thick sapphire windows. Light microscopy using a high-pressure diamond cell was applied to visualize formation and dissolution of protein droplets on the micrometer scale (see the SI for experimental details).

It was previously shown that LLPS of the SynGAP/PSD-95 system occurs at protein concentrations beyond 20 μM, and a temperature-dependent investigation of the SynGAP/PSD-95 system from 4 to 70 °C showed no significant temperature effect on the phase behavior.[27] Figure 1 depicts the effect of TMAO, urea, and Ficoll on the pressure-dependent phase behavior of SynGAP/PSD-95 using turbidity measurements. We observed the expected decrease in turbidity of the solution at a high pressure (Figure 1), indicating the disappearance of the droplet phase, which occurred at ~300 bar for the SynGAP/PSD-95 system in pure buffer solution at T = 25 °C.

As also seen in Figure 1, the cosolvents have a dramatic effect on the formation and pressure stability of the phase-separated state. Addition of 0.5 M TMAO shifts the overall transition to the homogeneous phase from ~300 bar to above 1 kbar. In contrast, 0.2 M urea causes a shift of the phase transition to lower pressures (~100 bar). Similar to TMAO, Ficoll imposes a stabilizing effect on the droplet phase of SynGAP/PSD-95, which is most likely due to the excluded volume effect favoring compact structures, which include protein-rich droplets. Remarkably, at a macromolecular crowder concentration as low as 7.5 wt % Ficoll, which is far below a typical macromolecular crowding situation inside a biological cell (~20–30 wt %), the overall transition to the homogeneous phase is already shifted to pressures of about 1 kbar.

To visualize the pressure- and cosolvent-dependent phase behavior of the SynGAP/PSD-95 system, light microscopy studies were performed. Figure 2 shows selected light microscopy snapshots of SynGAP/PSD-95 in pure buffer, 0.2 M TMAO, and 5 wt % Ficoll at T = 25 °C, representing the phase-separated state and the homogeneous state of the solution, depending on pressure. The results from the light microscopy images are in good agreement with those obtained from the turbidity measurements regarding the location of the LLPS stability region.
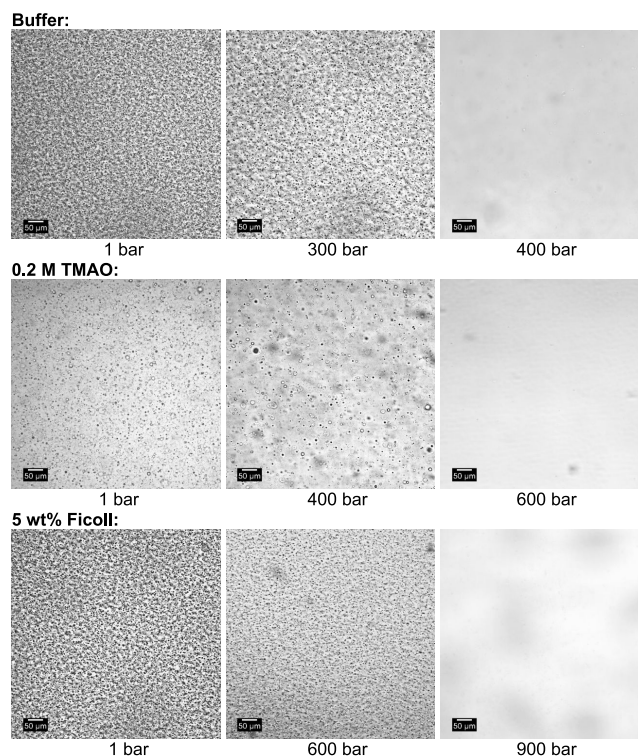
Figure 2. Light microscopy snapshots of the SynGAP/PSD-95 system in pure buffer, 0.2 M TMAO, and 5 wt % Ficoll at T = 25 °C, representing the phase-separated and homogeneous states of the SynGAP/PSD-95 mixture, depending on the pressure.

2.2. Steady-State Fluorescence Spectroscopy: Evaluation of the SynGAP—PSD-95 Binding Constants under Different Solution Conditions. To gain insights into the mechanisms by which cosolvents impact pressure-induced dissolution of the droplet phase of SynGAP and PSD-95, steady-state fluorescence spectroscopy was employed to determine the dissociation constant, K_d, of the SynGAP—PSD-95 complex. To this end, a solution of Alexa405-labeled PSD-95 (PSD-Alexa) was titrated with a solution of SynGAP. The extent of complex formation was then evaluated by monitoring the changes in the fluorescence intensity of PSD-Alexa. The binding isotherms were obtained by plotting F_0/F vs the total SynGAP concentration, $[\text{SynGAP}]_{\text{total}}$, and fitting the experimental data with a 1:1 binding model. Figure 3 shows the binding isotherms obtained at ambient temperature (25 °C) and selected pressures in neat buffer, in 0.5 M TMAO, and in 7.5 wt % Ficoll solution. All ambient pressure data, including those of the 0.2 M urea solution, are compared in Figure S1, and the binding curves in the presence of TMAO and Ficoll for all pressures recorded (500, 1000, 1500, and 2000 bar) are shown in Figures S2 and S3. All K_d values we measured are reported in Table 1.

The dissociation constant for the SynGAP—PSD-95 complex formation in neat buffer has been measured previously by the FRET methodology. K_d was found to be 1.7 μM at T = 25 °C and p = 1 bar.[27] The corresponding binding curve in the present experiment is reported in panel (a) of Figure 3. Data analysis yielded a K_d of 5.3 ± 1.5 μM, in rather good agreement with the previously reported value in view of the different methodologies used in the two measurements. The dissociation constant was also evaluated at a pressure of 2000 bar, and a value of K_d = 8.8 ± 1.8 μM was
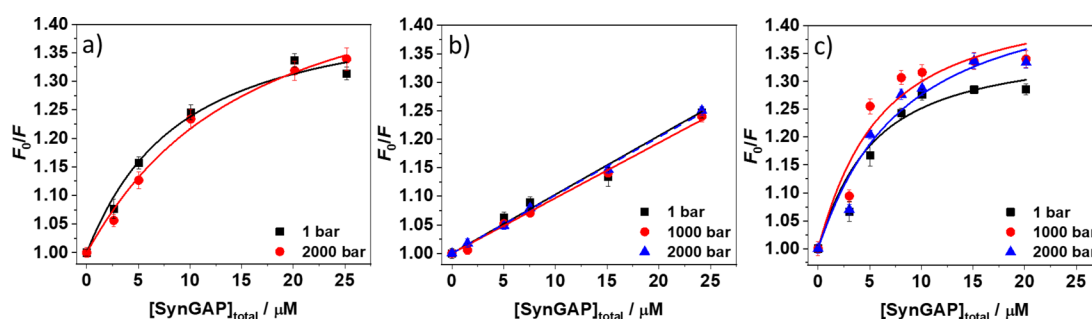
Figure 3. Binding isotherms for the complex formation between SynGAP and PSD-95 at $T = 25$ °C and at the indicated pressures in (a) 50 mM Tris−HCl buffer, 100 mM NaCl, 1 mM EDTA, 1 mM TCEP, pH 7.5; (b) in the same buffer with the addition of 0.5 M TMAO; and (c) in buffer with the addition of 7.5 wt % Ficoll. The experimental data, F_0/F vs [SynGAP]$_{\text{total}}$, were fitted accordingly to a 1:1 binding model equation in order to evaluate the dissociation constant, K_d.

Table 1. Dissociation Constants, K_d, for the Complex Formation between PSD-95 and SynGAP Obtained in the Reported Media at 25 °C and the Indicated Pressures

solvent	pressure (bar)	K_d (μM)
50 mM Tris−HCl, 100 mM NaCl	1	5.3 ± 1.5
	2000	8.8 ± 1.8
+ 0.5 M TMAO	1	99 ± 5.0
	500	100 ± 3.8
	1000	104 ± 2.3
	1500	104 ± 2.5
	2000	100 ± 1.4
+7.5 wt % Ficoll	1	6.2 ± 3.2
	500	5.5 ± 3.9
	1000	4.6 ± 2.6
	1500	4.2 ± 1.9
	2000	6.6 ± 3.2

obtained. This indicates, as previously observed, that pressurization may lead to only a small increase in K_d, i.e., SynGAP−PSD-95 complex formation in dilute solution in neat buffer is almost pressure insensitive. Nonetheless, the small increase in K_d with the increasing pressure in neat buffer does correlate with decreasing LLPS propensity with the increasing pressure, indicating that the pressure-dependent stability of the SynGAP−PSD-95 condensate is reflected by the strength of the dilute-phase pairwise SynGAP−PSD-95 interaction in neat buffer.[27] In contrast, when 0.5 M TMAO was added to the buffer, there was a significant increase in K_d. At 1 bar, the K_d is 99 μM, which is almost 20 times that in neat buffer, meaning that the favorable interaction between SynGAP and PSD-95 in the dilute phase is severely hampered by TMAO. Such behavior might originate in TMAO's effect of increasing the hydrogen-bonding network structure of water and the stability of the hydration layer around proteins in TMAO-water solutions.[35−38] TMAO interacts differently with different chemical groups of a protein chain.[44] Recent studies suggested that TMAO can be slightly accumulated near nonpolar groups while being strongly depleted from the amide groups of protein molecules, and thus the depletion of TMAO around protein molecules is highly sensitive to the configurations of the molecules.[45,46] In this perspective, the surprising large increase in K_d with addition of TMAO observed here implies that TMAO is relatively more depleted from the pairwise SynGAP−PSD-95 complex than from the free (uncomplexed) SynGAP and PSD-95 molecules, which is a possible scenario since TMAO has different aversions/

affinities for different chemical groups of the two proteins. Increasing the pressure up to 2000 bar does not affect the high K_d value significantly (Table 1). Despite the destabilization of the pairwise SynGAP−PSD-95 complex by TMAO, the dense droplet phase of SynGAP and PSD-95 is stabilized in the TMAO-containing solution relative to that in neat buffer for all pressures we studied (Figure 1), suggesting that TMAO is less depleted from the droplet boundary, leading to the observed stabilization of the droplet phase against pressure. Taken together, the seemingly divergent effects of TMAO on pairwise SynGAP−PSD-95 association and SynGAP/PSD-95 phase separation indicate that the stabilization of the SynGAP/PSD-95 condensate by TMAO is operating on higher-order (many-body) interactions rather than at the pairwise (two-body) level. This observation is consistent with the recent finding that SynGAP/PSD-95 condensates are stabilized by additional interactions auxiliary to those manifested in the dilute phase.[47]

When the denaturing agent urea at the concentration 0.2 M was added to the buffer, there were only very small changes in the fluorescence intensity of PSD-Alexa upon addition of SynGAP (up to ~25 μM) and no binding curve could be obtained (Figure S1). These findings are a clear indication that when urea is present in solution, the formation of the complex is so severely diminished that no binding was observed. In contrast to the above observations for TMAO, the urea-induced diminishing of dilute-phase SynGAP−PSD-95 binding is correlated with the destabilization of the droplet phase by urea, as one might expect intuitively. Increasing the pressure up to 2000 bar does not lead to any changes in behavior (data not shown). As urea is known to interact with the backbone and side chains of proteins in a manner that favors the unfolded state, the same types of interactions are probably also responsible for the observed urea-induced decrease in droplet stability upon compression (Figure 1a).

In the presence of 7.5 wt % of the crowding agent Ficoll, a K_d value of 6.2 ± 3.2 μM was determined, which is similar to that in neat buffer (Table 1). Thus, the presence of Ficoll apparently has no significant effect on the favorability of pairwise complex formation between PSD-95 and SynGAP in dilute solution. Upon pressurization of the system, no significant changes in K_d were observed either. One may therefore surmise that Ficoll induces the striking stabilization of the droplet phase (Figure 1) by an entropic excluded volume effect that favors the droplet phase of SynGAP/PSD-95 because the condensate's compactness entails a lower solvent-excluded volume.

2.3. Pressure-Jump Relaxation Kinetics: The Time-scales of Formation and Dissolution of the LLPS State. Besides conducting equilibrium measurements under different pressures to mimic conditions experienced by deep-sea organisms as reported above, we have also utilized pressure as a physical probe to study LLPS kinetics. Figure 4a depicts the time-dependent absorbance data of SynGAP/PSD-95 at a concentration of 50 μM (1:1 molar ratio) at room temperature
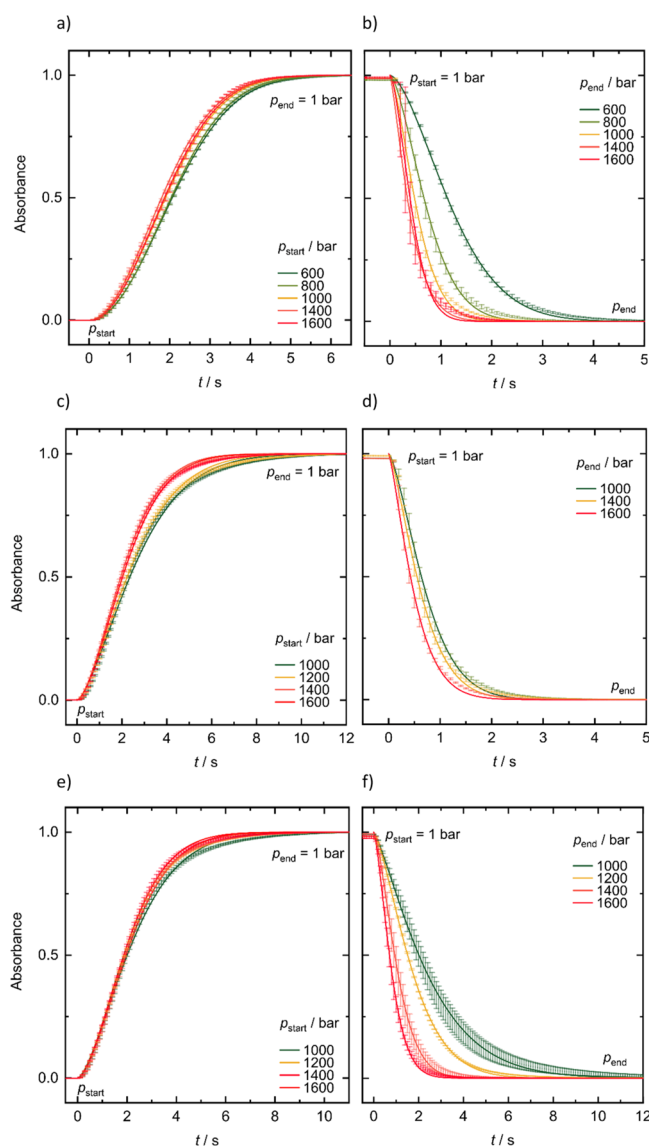
Figure 4. Time course of the absorption (turbidity), $A(t)$, of a 50 μM SynGAP/PSD-95 solution in (a, b) neat buffer, (c, d) 0.2 M TMAO, and (e, f) 5 wt % Ficoll at T = 20 °C after rapid pressure-jumps of variable amplitudes, from high pressure to ambient pressure (depressurization, LLPS formation, panels on the left), and from 1 bar to high pressure (pressurization, vanishing of the two-phase region, panels on the right). The absorption data were normalized to their maximum values (absorbance = 1.0); an absorbance of ~1 signifies the phase-separated equilibrium state of SynGAP/PSD-95 in the LLPS state at ambient pressure (1 bar). Results of further concentrations measured can be found in the SI. Concentrations beyond 0.3 M TMAO could not be measured in the kinetics experiments because rapid droplet condensation and precipitation of droplets in the UV/Vis sample cell prohibited us from taking accurate turbidity data.

(25 °C) following a rapid (~50 ms) pressure-jump at time t = 0 from different pressures above 600 bar to ambient pressure (1 bar), i.e., the jump is in the depressurizing, LLPS-favoring direction. As expected, the absorbance increases rapidly upon entering the LLPS region from the homogeneous phase and flattens out after about 6.4 s when an equilibrium state is reached. Figure 4b shows the pressure-jump data in the opposite, i.e., pressurization direction, revealing a disassembly kinetics, which is about three times faster than the droplet formation kinetics in Figure 4a. Nonetheless, in both pressure-jump directions, the overall transition time is fast. The processes all occur on the seconds' time scale, with the transition time decreasing slightly with the increasing amplitude of the pressure jump.

To quantify the kinetics data, the kinetic profiles were fitted to the Johnson–Mehl–Avrami–Kolmogorov (JMAK) function:[49−51] $A(t) = 1 - \exp(-kt^n)$ when entering the LLPS region and $A(t) = \exp(-kt^n)$ when entering the homogeneous phase; n is the Avrami exponent, and k an apparent rate constant; $A(t)$ is proportional to the time-dependent volume fraction, V_{droplet}/V, of the condensed droplet phase. From the time-lapse kinetic data, the total transition time, t_{tr}, i.e., the time for completion of the phase transition and reaching an equilibrium state, and the half-life time, $t_{1/2}$, i.e., the time to reach half of the absorption intensity changes, were determined (Tables S1−4).

An Avrami exponent of $n \approx 2$ was determined, which suggests that LLPS formation proceeds via a diffusion-limited nucleation and growth mechanism. Avrami exponents between $n \approx 1.5$ and $n \approx 2.5$ indicate a nucleation/growth regime consistent with mixed heterogeneous ($n \approx 1.5$) and homogeneous ($n \approx 2$) nucleation. If diffusion zones of neighboring droplets start to overlap, then a crossover to an $n \approx 1$ regime may be observed, as seen for the highly concentrated (0.3 M) TMAO solution (Table S3).

As an example, Figure 4c,d depicts the absorbance data of SynGAP/PSD-95 upon addition of 0.2 M TMAO. The presence of 0.2 M TMAO results in a shift of the overall transition time for LLPS formation from ~6 to ~12 s (Table S2), while no significant effect of the cosolvent on the kinetics of dissolution of the two-phase region was observed. Upon addition of 0.3 M TMAO to the buffer, the overall transition time for LLPS formation shifted further to a longer time of ~40 s, i.e., the presence of TMAO retards LLPS formation significantly (Table S3). A similar trend was observed in the presence of 5 wt % of the macromolecular crowding agent Ficoll, although the effect was not as pronounced as with TMAO (Figure 4e,f).

3. DISCUSSION AND CONCLUSIONS

In this study, we explored the effect of cosolvents and a macromolecular crowding agent on liquid-phase droplets and the LLPS kinetics of two major components of PSDs, SynGAP and PSD-95. PSDs concentrate receptors of neurotransmitters and serve as a signaling machinery in response to synaptic activities, exchanging components with the surrounding cytoplasm and being altered by synaptic plasticity.[21,22,53] It has been shown that the liquid phase droplets of the SynGAP/PSD-95 model system for PSDs are among the most pressure-sensitive biomolecular assemblies identified to date. Increasing the pressure by several ten to hundred bar leads to a dramatic decrease in droplet stability with the disappearance of phase separation for the 50 μM SynGAP/PSD-95 model system at

about 200 bar. Accordingly, the critical pressure of the PSD-mimicking SynGAP/PSD-95 system is more than an order of magnitude smaller compared to those typically required for protein unfolding or unfolding of canonical nucleic acid structures.[1,2,5,7,54,55] The extreme pressure sensitivity of the SynGAP/PSD-95 system suggests a very large partial molar volume difference of the proteins in the droplet relative to the state when they are free in solution. This may involve the associated or dissociated states of the two proteins and, probably, may also reflect the properties and amount of water of hydration of the proteins in the droplet and in the bulk. Since the pressure dependence of pairwise SynGAP—PSD-95 association is not sufficient to explain the observed pressure sensitivity of the SynGAP/PSD-95 droplets, a reasonable physical explanation is that a substantial void volume inaccessible to water molecules is associated with the multiple-molecule interaction network in the dense droplet phase compared with the dilute solution phase of SynGAP/PSD-95, resulting in an overall decrease in the volume of the system upon dissociation of the droplet phase.[27]

A major finding here is that the compatible osmolyte TMAO at moderate concentrations can mitigate the deleterious effect of pressure on droplet stability, making the SynGAP/PSD-95 condensate model of PSD stable up to almost the kbar level (the average pressure in the world's oceans is ∼400 bar, and a maximum pressure of ∼1100 bar is experienced in the Mariana trench). Macromolecular crowding, a ubiquitous thermodynamic force in the cellular environment, as mimicked here by the biocompatible polysaccharide Ficoll, also exhibited a similar strong stabilizing effect on the droplet phase of SynGAP/PSD-95. The net impact of a crowder may be interpreted as amounting to an effective enhancement of protein—protein interactions promoted by the crowder's excluded volume.

Apparently, TMAO contributes to piezophilic metabolism and likely serves to protect proteins from the detrimental effects of high pressure.[12,33,34] Consistent with this expectation, the amount of TMAO in the cells of a series of marine organisms was found to increase linearly with ocean depth, up to a concentration of about 0.5 M, which is the maximum TMAO concentration considered in the present work. Indeed, Treberg et al.[56] have shown further that not only is the TMAO content increasing in muscle cells of fish caught from increasing depths in the deep ocean but an accumulation of TMAO is also observed in various other tissues of teleosts, including the brain. Moreover, the concentration of TMAO in deep-water species can be up to two orders of magnitude higher than that in shallow-water species. The present results indicate that organisms may use stabilizing osmolytes such as TMAO and cellular crowding not only to compensate for extreme environmental conditions and to protect individual protein molecules from unfolding and denaturation, but they may also use these same cosolutes to maintain and control biomolecular LLPS processes that are critical to life's function under high-pressure stress. Aside from the stabilization effects of such cosolutes, sequence variations of proteins could also contribute to adaptation under high hydrostatic pressure, similar to proteins in thermophiles adapted to life at high temperatures. However, no such information is available to date. Future efforts should be undertaken to address this question.

Owing to its large dipole moment, TMAO has the ability to strongly interact with water and there seems to be consensus that TMAO generally does not bind preferentially to protein surfaces,[32,35−38] though some studies suggested that TMAO can be slightly attracted to the nonpolar groups in proteins.[45,46] This seems to be also the reason for the strong stabilization of the droplet phase as observed here, which is likely largely devoid of a cosolvent. TMAO has been proposed to serve as an anchor point from which the tetrahedral network of water can build and become more stable, and TMAO is believed to be capable of resisting the pressure-induced structural perturbation of water.[38] It follows that the TMAO-induced increase in hydrogen bonding of the water structure opposes the penetration of water into the voids within compact folded protein structures, thus rendering a major process of volume decrease that favors protein unfolding at high pressures less likely.[52] A similar scenario may also apply to the dense droplet phase of SynGAP/PSD-95 as part of TMAO's stabilizing effects on the condensed phase.

Our pressure-jump experiments indicate that the formation of the droplet phase of SynGAP/PSD-95 is a very rapid process that can be switched on and off on the few-seconds' timescale. Compared to the prominent effect of the TMAO and Ficoll cosolutes on the stability of the LLPS state, their effect at biologically relevant concentrations on the phase separation kinetics is rather small, which might turn out to be functionally advantageous in the cellular context because in that case, the fast assembly—disassembly switching capability of the droplet-like membraneless organelle would not be compromised by the presence of cellular cosolutes. Among the TMAO concentrations we considered, only a high concentration of 0.3 M leads to an approximately 10-fold increase in LLPS time. In other words, the strongly stabilizing compatible osmolyte TMAO can delay droplet formation at high concentrations, which, together with its pronounced effect on droplet stability, could affect the plasticity of PSDs and thus affect—even severely compromise—their function in neurons. However, in view of the rudimentary nature of the SynGAP/PSD-95 condensate model for PSD, to elucidate the structure—function relationship of PSDs under high-pressure-cosolvent conditions, further efforts such as preparation and utilization of more sophisticated in vitro PSD models[22] in pressure- and cosolvent-dependent experiments will be needed.

The stability of the nervous system of deep-sea organisms (e.g., elasmobranchs or teleosts like the hadal snailfish, which thrives at ocean depths up to 7000 m) at a high pressure is an important yet given fact of their evolution. However, air-breathing human divers face a dramatic version of changes in motor function and nervous system excitability as documented by the pathologies of HPNS.[15] Comparative physiological, biochemical, and biophysical studies of high-pressure adaptation of the nervous system awaits further concerted investigations. The present observation of the effect of pressure on the LLPS of the simple SynGAP/PSD-95 model of PSD offers new biophysical insights into neurological effects of hydrostatic pressure and how particular cosolutes of the cellular milieu, such as TMAO, might mitigate deleterious effects of pressure. Since properly regulated assembly and partial disassembly of PSDs are crucial for neurological function,[57,58] our findings here may help in unraveling the underlying mechanisms of neurological disorders in organisms exposed to high hydrostatic pressures as well as the effects of ingesting high concentrations of TMAO on neuronal dysfunction by probably impairing the plasticity of PSDs.

■ ASSOCIATED CONTENT

ⓈⒾ Supporting Information

The Supporting Information is available free of charge at https://pubs.acs.org/doi/10.1021/acs.jpcb.2c00794.

> Sample preparation; methods; binding isotherms for the complex formation between PSD-95 and SynGAP at a temperature of 25 °C and pressure of 1 bar in 50 mM Tris-HCl buffer, 100 mM NaCl, 1 mM EDTA, and 1 mM TCEP, pH 7.5; in the same buffer with the addition of 0.5 M TMAO; and in buffer with the addition of 0.2 M urea; in buffer with the addition of 7.5 wt % Ficoll; binding isotherms for the complex formation between PSD-95 and SynGAP at a temperature of 25 °C in the presence of 0.5 M TMAO at the pressures of 500, 1000, 1500, and 2000 bar; binding isotherms for the complex formation between PSD-95 and SynGAP at a temperature of 25 °C in the presence of 7.5 wt % Ficoll at the pressure of 500, 1000, 1500, and 2000 bar; and kinetic parameters obtained from the fits to the Johnson−Mehl−Avrami−Kolmogorov function to yield the Avrami exponent, n, and rate constant, k (PDF)

■ AUTHOR INFORMATION

Corresponding Author

Roland Winter − *Physical Chemistry I - Biophysical Chemistry, Department of Chemistry and Chemical Biology, TU Dortmund University, 44227 Dortmund, Germany;* ⓞ orcid.org/0000-0002-3512-6928; Email: roland.winter@tu-dortmund.de

Authors

Hasan Cinar − *Physical Chemistry I - Biophysical Chemistry, Department of Chemistry and Chemical Biology, TU Dortmund University, 44227 Dortmund, Germany*

Rosario Oliva − *Physical Chemistry I - Biophysical Chemistry, Department of Chemistry and Chemical Biology, TU Dortmund University, 44227 Dortmund, Germany*

Haowei Wu − *Division of Life Science, State Key Laboratory of Molecular Neuroscience, Hong Kong University of Science and Technology, Kowloon 999077, China*

Mingjie Zhang − *Division of Life Science, State Key Laboratory of Molecular Neuroscience, Hong Kong University of Science and Technology, Kowloon 999077, China; School of Life Sciences, Southern University of Science and Technology, Shenzhen 518055, China;* ⓞ orcid.org/0000-0001-9404-0190

Hue Sun Chan − *Department of Biochemistry, Faculty of Medicine, University of Toronto, Toronto, Ontario M5S 1A8, Canada;* ⓞ orcid.org/0000-0002-1381-923X

Complete contact information is available at:
https://pubs.acs.org/10.1021/acs.jpcb.2c00794

Notes

The authors declare no competing financial interest.

■ ACKNOWLEDGMENTS

■ REFERENCES

(1) Akasaka, K.; Matsuki, H. Eds., *High Pressure Bioscience. Basic Concepts, Applications and Frontiers*; Springer, 2015.

(2) Silva, J. L.; Oliveira, A. C.; Vieira, T. C. R. G.; de Oliveira, G. A. P.; Suarez, M. C.; Foguel, D. High-pressure chemical biology and biotechnology. *Chem. Rev.* **2014**, *114*, 7239−7267.

(3) Mishra, R.; Winter, R. Cold- and pressure-induced dissociation of protein aggregates and amyloid fibrils. *Angew. Chem., Int. Ed.* **2008**, *47*, 6518−6521.

(4) Roche, J.; Caro, J. A.; Norberto, D. R.; Barthe, P.; Roumestand, C.; Schlessman, J. L.; Garcia, A. E.; García-Moreno, B. E.; Royer, C. A. Cavities determine the pressure unfolding of proteins. *Proc. Natl. Acad. Sci. U. S. A.* **2012**, *109*, 6945−6950.

(5) Winter, R. Interrogating the structural dynamics and energetics of biomolecular systems with pressure modulation. *Annu. Rev. Biophys.* **2019**, *48*, 441−463.

(6) Fan, H. Y.; Shek, Y. L.; Amiri, A.; Dubins, D. N.; Heerklotz, H.; Macgregor, R. B., Jr.; Chalikian, T. Volumetric characterization of sodium-induced G-quadruplex formation. *J. Am. Chem. Soc.* **2011**, *133*, 4518−4526.

(7) Heremans, K.; Smeller, L. Protein structure and dynamics at high pressure. *Biochim. Biophys. Acta* **1998**, *1386*, 353−370.

(8) Kalbitzer, H. R. High pressure NMR methods for characterizing functional substates of proteins. *High Pressure Biosci.* **2015**, *72*, 179−197.

(9) Kapoor, S.; Triola, G.; Vetter, I. R.; Erlkamp, M.; Waldmann, H.; Winter, R. Revealing conformational substates of lipidated N-Ras protein by pressure modulation. *Proc. Natl. Acad. Sci. U. S. A.* **2012**, *109*, 460−465.

(10) Daniel, I.; Oger, P.; Winter, R. Origins of life and biochemistry under high-pressure conditions. *Chem. Soc. Rev.* **2006**, *35*, 858−875.

(11) Meersman, F.; Daniel, I.; Bartlett, D.; Winter, R.; Hazael, R.; McMillan, P. F. High-pressure biochemistry and biophysics. *Rev. Mineral. Geochem.* **2013**, *75*, 607−648.

(12) Macdonald, A. *Life at high pressure*; Springer International Publishing, 2021.

(13) Sébert, P. Ed., *Comparative High Pressure Biology*; Science Publishers, 2010.

(14) Jannasch, H. W.; Marquis, R. E.; Zimmermann, A. M. Eds., *Current Perspectives in High Pressure Biology*; Academic Press, 1987.

(15) Talpalar, A. E. High pressure neurological syndrome. *Rev. Neurol.* **2007**, *45*, 631−636.

(16) Brangwynne, C. P.; Tompa, P.; Pappu, R. V. Polymer physics of intracellular phase transitions. *Nat. Phys.* **2015**, *11*, 899−904.

(17) Banani, S. F.; Lee, H. O.; Hyman, A. A.; Rosen, M. K. Biomolecular condensates: organizers of cellular biochemistry. *Nat. Rev. Mol. Cell Biol.* **2017**, *18*, 285−298.

(18) Brady, J. P.; Farber, P. J.; Sekhar, A.; Lin, Y.-H.; Huang, R.; Bah, A.; Nott, T. J.; Chan, H. S.; Baldwin, A. J.; Forman-Kay, J. D.; Kay, L. E. Structural and hydrodynamic properties of an intrinsically disordered region of a germ cell-specific protein on phase separation. *Proc. Natl. Acad. Sci. U. S. A.* **2017**, *114*, E8194−E8203.

(19) Lin, Y.-H.; Forman-Kay, J. D.; Chan, H. S. Theories for sequence-dependent phase behaviors of biomolecular condensates. *Biochemistry* **2018**, *57*, 2499−2508.

(20) Cinar, H.; Fetahaj, Z.; Cinar, S.; Vernon, R. M.; Chan, H. S.; Winter, R. Temperature, hydrostatic pressure, and osmolyte effects on liquid-liquid phase separation in protein condensates: physical chemistry and biological implications. *Chem. − Eur. J.* **2019**, *25*, 13049−13069.

(21) Zeng, M.; Shang, Y.; Araki, Y.; Guo, T.; Huganir, R. L.; Zhang, M. Phase transition in postsynaptic densities underlies formation of

synaptic complexes and synaptic plasticity. *Cell* **2016**, *166*, 1163−1175.e12.

(22) Zeng, M.; Chen, X.; Guan, D.; Xu, J.; Wu, H.; Tong, P.; Zhang, M. Reconstituted postsynaptic density as a molecular platform for understanding synapse formation and plasticity. *Cell* **2018**, *174*, 1172−1187.e16.

(23) Chen, X.; Wu, X.; Wu, H.; Zhang, M. Phase separation at the synapse. *Nat. Neurosci.* **2020**, *23*, 301−310.

(24) Zeng, M.; Ye, F.; Xu, J.; Zhang, M. PDZ ligand binding-induced conformational coupling of the PDZ−SH3−GK tandems in PSD-95 family MAGUKs. *J. Mol. Biol.* **2018**, *430*, 69−86.

(25) Julius, K.; Weine, J.; Berghaus, M.; König, N.; Gao, M.; Latarius, J.; Paulus, M.; Schroer, M. A.; Tolan, M.; Winter, R. Water-mediated protein-protein interactions at high pressures are controlled by a deep-sea osmolyte. *Phys. Rev. Lett.* **2018**, *121*, No. 038101.

(26) Cinar, H.; Cinar, S.; Chan, H. S.; Winter, R. Pressure-induced dissolution and reentrant formation of condensed, liquid-liquid phase-separated elastomeric α-elastin. *Chem. − Eur. J.* **2018**, *24*, 8286−8291.

(27) Cinar, H.; Oliva, R.; Lin, Y.; Chen, X.; Zhang, M.; Chan, H. S.; Winter, R. Pressure sensitivity of SynGAP—PSD-95 condensates as a model for postsynaptic densities and its biophysical and neurological ramifications. *Chem. − Eur. J.* **2020**, *26*, 11024−11031.

(28) Cinar, H.; Cinar, S.; Chan, H. S.; Winter, R. Pressure-sensitive and osmolyte-modulated liquid-liquid phase separation of eye-lens γ-crystallins. *J. Am. Chem. Soc.* **2019**, *141*, 7347−7354.

(29) Li, S.; Yoshizawa, T.; Yamazaki, R.; Fujiwara, A.; Kameda, T.; Kitahara, R. Pressure and temperature phase diagram for liquid-liquid phase separation of the RNA-binding protein fused in sarcoma. *J. Phys. Chem. B* **2021**, *125*, 6821−6829.

(30) Kitahara, R.; Yamazaki, R.; Ide, F.; Li, S.; Shiramasa, Y.; Sasahara, N.; Yoshizawa, T. Pressure-jump kinetics of liquid-liquid phase separation: comparison of two different condensed phases of the RNA-binding protein, fused in sarcoma. *J. Am. Chem. Soc.* **2021**, *143*, 19697−19702.

(31) Zhou, H.-X.; Rivas, G.; Minton, A. P. Macromolecular crowding and confinement: biochemical, biophysical, and potential physiological consequences. *Annu. Rev. Biophys.* **2008**, *37*, 375−397.

(32) Gao, M.; Held, C.; Patra, S.; Arns, L.; Sadowski, G.; Winter, R. Crowders and cosolvents-major contributors to the cellular milieu and efficient means to counteract environmental stresses. *ChemPhysChem* **2017**, *18*, 2951−2972.

(33) Yancey, P. H. Organic osmolytes as compatible, metabolic and counteracting cytoprotectants in high osmolarity and other stresses. *J. Exp. Biol.* **2005**, *208*, 2819−2830.

(34) Yancey, P. H. Cellular responses in marine animals to hydrostatic pressure. *J. Exp. Zool., Part A* **2020**, *333*, 398−420.

(35) Canchi, D. R.; García, A. E. Cosolvent effects on protein stability. *Annu. Rev. Phys. Chem.* **2013**, *64*, 273−293.

(36) Julius, K.; Weine, J.; Latarius, J.; Elbers, M.; Paulus, M.; Tolan, M.; Winter, R. Impact of Macromolecular Crowding and Compression on Protein-Protein Interactions and Liquid-Liquid Phase Separation Phenomena. *Macromolecules* **2019**, *52*, 772−1784.

(37) Hölzl, C.; Kibies, P.; Imoto, S.; Frach, R.; Suladze, S.; Winter, R.; Marx, D.; Horinek, D.; Kast, S. M. Design principles for high-pressure force fields: aqueous TMAO solutions from ambient to kilobar pressures. *J. Chem. Phys.* **2016**, *144*, 144104−144116.

(38) Laurent, H.; Baker, D. L.; Soper, A. K.; Ries, M. E.; Dougan, L. Solute specific perturbations to water structure and dynamics in tertiary aqueous solution. *J. Phys. Chem. B* **2020**, *124*, 10983−10993.

(39) Su, Z.; Dias, C. L. Individual and combined effects of urea and trimethylamine N-oxide (TMAO) on protein structures. *J. Mol. Liq.* **2019**, *293*, 111443.

(40) Ganguly, P.; Polaók, J.; van der Vegt, N. F. A.; Heyda, J.; Shea, J.-E. Protein stability in TMAO and mixed urea-TMAO solutions. *J. Phys. Chem. B* **2020**, *124*, 6181−6197.

(41) Govindarajulu, M.; Pinky, P. D.; Steinke, I.; Bloemer, J.; Ramesh, S.; Kariharan, T.; Rella, R. T.; Bhattacharya, S.; Dhanasekaran, M.; Suppiramaniam, V.; Amin, R. H. Gut metabolite TMAO induces synaptic plasticity deficits by promoting endoplasmic reticulum stress. *Front. Mol. Neurosci.* **2020**, *13*, 138.

(42) Chen, L.; Chen, Y.; Zhao, M.; Zheng, L.; Fan, D. Changes in the concentrations of trimethylamine N-oxide (TMAO) and its precursors in patients with amyotrophic lateral sclerosis. *Sci. Rep.* **2020**, *10*, 15198.

(43) Li, D.; Ke, Y.; Zhan, R.; Liu, C.; Zhao, M.; Zeng, A.; Shi, X.; Ji, L.; Cheng, S.; Pan, B.; et al. Trimethylamine-N-oxide promotes brain aging and cognitive impairment in mice. *Aging Cell* **2018**, *17*, No. e12768.

(44) Cho, S. S.; Reddy, G.; Straub, J. E.; Thirumalai, D. Entropic stabilization of proteins by TMAO. *J. Phys. Chem. B* **2011**, *115*, 13401−13407.

(45) Mondal, J.; Halverson, D.; Li, I. T. S.; Stirnemann, G.; Walker, G. C.; Berne, B. J. How osmolytes influence hydrophobic polymer conformations: A unified view from experiment and theory. *Proc. Natl. Acad. Sci. U. S. A.* **2015**, *112*, 9270−9275.

(46) Liao, Y.-T.; Manson, A. C.; DeLyser, M. R.; Noid, W. G.; Cremer, P. S. Trimethylamine N-oxide stabilizes proteins via a distinct mechanism compared with betaine and glycine. *Proc. Natl. Acad. Sci. U. S. A.* **2017**, *114*, 2479−2484.

(47) Lin, Y.-H.; Wu, H.; Jia, B.; Zhang, M.; Chan, H. S. Assembly of model postsynaptic densities involves interactions auxiliary to stoichiometric binding. *Biophys. J.* **2022**, *121*, 157−171.

(48) Cinar, H.; Winter, R. The effects of cosolutes and crowding on the kinetics of protein condensate formation based on liquid-liquid phase separation - a pressure-jump relaxation study. *Sci. Rep.* **2020**, *10*, 17245.

(49) Papon, P.; Leblond, J.; Meijer, P. H. E. *The Physics of Phase Transitions*; Springer, 2006.

(50) Avrami, M. Kinetics of phase change I. General theory. *J. Chem. Phys.* **1939**, *7*, 1103−1112.

(51) Avrami, M. Kinetics of phase change. II. Transformation time relations for random distribution of nuclei. *J. Chem. Phys.* **1940**, *8*, 212−224.

(52) Royer, C. A. Revisiting volume changes in pressure-induced protein unfolding. *Biochim. Biophys. Acta* **2002**, *1595*, 201−209.

(53) Ryan, H.; Fawzi, N. L. Physiological, pathological, and targetable membraneless organelles in neurons. *Trends Neurosci.* **2019**, *42*, 693−708.

(54) Takahashi, S.; Sugimoto, N. Effect of pressure on thermal stability of G-quadruplex DNA and double-stranded DNA structures. *Molecules* **2013**, *18*, 13297−13319.

(55) Knop, J.-M.; Patra, S.; Harish, B.; Royer, C. A.; Winter, R. The deep sea osmolyte trimethylamine N-oxide and macromolecular crowders rescue the antiparallel conformation of the human telomeric G-quadruplex from urea and pressure stress. *Chem. − Eur. J.* **2018**, *24*, 14346−14351.

(56) Treberg, J. R.; Driedzic, W. R. Elevated Levels of Trimethyl-amine Oxide in Deep-Sea Fish: Evidence for Synthesis and Intertissue Physiological Importance. *J. Exp. Zool.* **2002**, *293*, 39−45.

(57) de Vivo, L.; Bellesi, M.; Marshall, W.; Bushong, E. A.; Ellisman, M. H.; Tononi, G.; Cirelli, C. Ultrastructural evidence for synaptic scaling across the wake/sleep cycle. *Science* **2017**, *355*, 507−510.

(58) Diering, G. H.; Nirujogi, R. S.; Roth, R. H.; Worley, P. F.; Pandey, A.; Huganir, R. L. Homer1a drives homeostatic scaling-down of excitatory synapses during sleep. *Science* **2017**, *355*, 511−515.